PHYSICAL REVIEW C VOLUME 11, NUMBER 5 MAY 1975

Barrier penetrability and/or deformation effects in ^{35}Cl induced fusion on ^{58,60,62,64}Ni

W. Scobel,* A. Mignerey, and M. Blann
Department of Chemistry and Nuclear Structure, Research Laboratory, University of Rochester, Rochester, New York 14627

H. H. Gutbrod
Gesellschaft für Schwerionenforschung, Darmstadt, Germany, and Brookhaven National Laboratory, Upton, New York 11973
(Received 6 February 1975)

Excitation functions for complete fusion have been measured for ^{35}Cl projectiles on ^{58,60,62,64}Ni. Deviations from the predictions of the sharp cutoff model are observed and compared with calculations based on the formalism of Wong. In this picture tunneling and static deformation of target and projectile can explain the experimental data in the barrier region.

[NUCLEAR REACTIONS complete fusion, ^{58,60,62,64}Ni + ^{35}Cl, E_{lab} = 91–170 MeV; measured $\sigma(\theta, E)$ for evaporation residues.]

I. INTRODUCTION

The increasing interest in the mechanism of heavy ion induced reactions has initiated many investigations on complete fusion during the last few years. Experimental results recently obtained at different laboratories, e.g. Orsay, Berkeley, Columbia, and Dubna, have focused attention mainly on fusion limits high above the interaction barrier. Thus the fusion barrier itself was somewhat neglected and data on its height, shape, and radius as a test for the existing theoretical predictions are scarce.

The precise determination of the barrier defining parameters requires the separation of the (classical) influence of target and projectile deformations from the quantum-mechanical effect of barrier penetrability. Both effects cause similar deviations from the behavior of purely classical, sticky, spherical nuclei. Accordingly, the analysis of the small amount of low energy fusion data and of total reaction cross sections near the barrier shows that it is difficult to isolate the relevant parameters.[1,2]

The experimental data to be reported here are part of an investigation of ^{35}Cl induced fusion on targets with masses between ^{27}Al and ^{124}Sn.[3] The fusion of ^{35}Cl with nickel isotopes was chosen for investigation of the fusion threshold region as it allows study of the transition from a nearly spherical nucleus, ^{58}Ni, to more deformed nuclei, ^{62,64}Ni, without changing the atomic number. Such a transition in the ground state deformation of the nickel isotopes is predicted by Hartree-Fock calculations.[4]

II. EXPERIMENTAL PROCEDURE AND RESULTS

The data presented in this paper were taken with special attention to good energy resolution by using electrostatic accelerators and thin targets. The ^{35}Cl beam was provided by the Rochester MP tandem Van de Graaff and the three stage MP tandem facility at Brookhaven National Laboratory. Self-supporting isotopically enriched Ni targets of 40–70 μg/cm^2 thickness and less than 0.1% contamination of the heavier nickel isotopes in each case were bombarded with ^{35}Cl ions with lab energies between 91 and 170 MeV. A typical energy loss in the targets at the lower projectile energies was about 600 keV. The center of mass energies given are corrected for this effect, taking into account the slope of the excitation functions $\sigma_{er}(E)$.

The evaporation residues (er) as well as the elastically scattered ^{35}Cl ions, Ni recoils, and transfer-reaction products were detected by two telescopes, each consisting of a ΔE proportional counter and a $(E-\Delta E)$ solid state detector. Beam position on target, beam intensity, and target thickness were monitored by two solid state counters mounted symmetrically with respect to the beam axis. The detector angle was thus defined to better than 0.2°. The acceptance angle was 0.5°, taking into account the beam size on target and the detector aperture. Further details of the experimental technique are given in Ref. 5.

Data were taken between 2.8 and 28° (lab) in 1 or 2° steps. The absolute differential cross sections for evaporation residues were derived by normalizing the relative cross sections to the simulta-

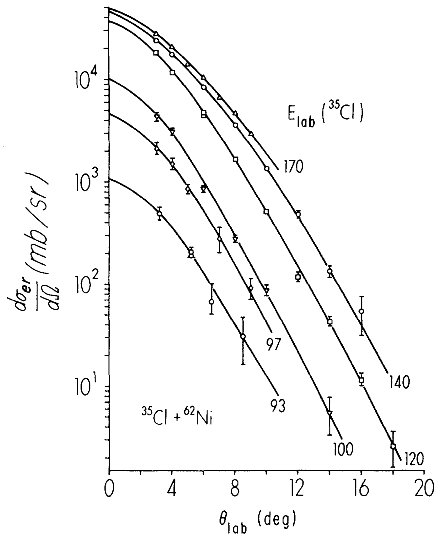

FIG. 1 Angular distribution of the evaporation residue cross section at various energies for the system ^{35}Cl + ^{62}Ni.

neously measured elastic scattering, which, in this angular region, is purely determined by Rutherford scattering. In Fig. 1, a representative set of angular distributions for the evaporation residue cross sections is shown for the reaction ^{35}Cl on ^{62}Ni at various energies. Integration over angle yields the total evaporation residue cross section. The extrapolation of the data into the 0–2.8° region sets the lower limit in the absolute error to 7–10%. Well above the barrier, the relative errors in the fusion excitation functions are only about 5%, due to the similar shapes of the angular distributions; at the lowest projectile energies they reach 20% due to the poorer statistics and the influence of target contaminations, whose influence was checked with runs well below the fusion barrier.

The resulting evaporation residue cross sections can be interpreted as complete fusion cross sections in the energy region considered. The resulting data are presented in Fig. 2 as a function of $E_{\mathrm{c.m.}}^{-1}$.

III. DISCUSSION

The analysis of the data in part follows a formalism described by Wong[6] for the reaction cross section. The cross section for complete fusion is given as

$$\sigma_{cf} = \pi \lambda\!\!\!^{-}{}^2 \sum_{l=0}^{l_{\mathrm{fus}}} (2l+1) T(l,E) , \tag{1}$$

where the energy dependent penetration factor $T(l, E)$ is approximated by the Hill-Wheeler formula[7] for the parabolic barrier

$$T(l,E) = \left[1 + \exp 2\pi \frac{E - V(R_l)}{\hbar \omega_l} \right]^{-1} . \tag{2}$$

We do not consider a lower cutoff for the partial fu-

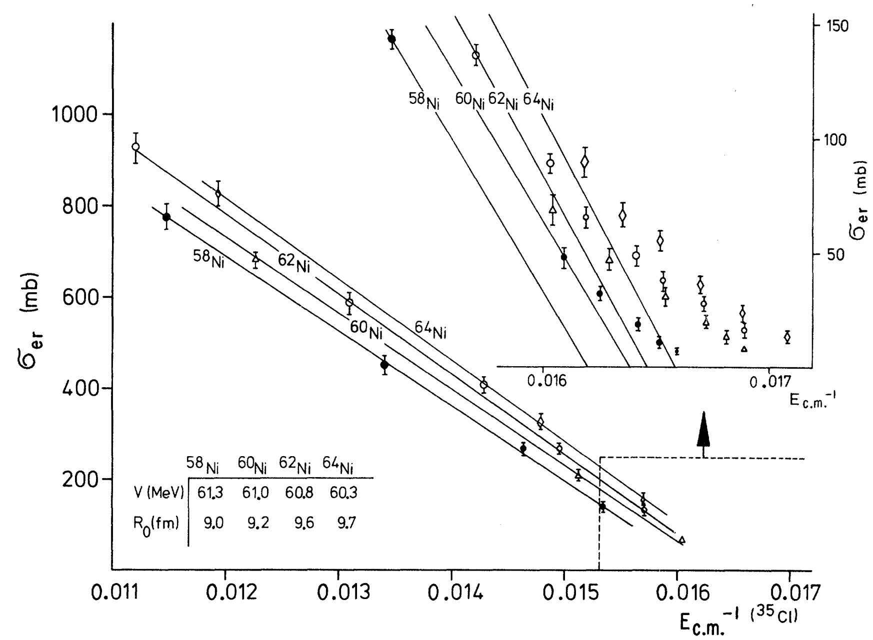

FIG. 2. Excitation function of complete fusion for ^{35}Cl on ^{58,60,62,64}Ni as a function of $E_{\mathrm{c.m.}}^{-1}$. Only relative errors are given. The straight lines are the results of Eq. (4) with the parameters taken from Table I.

TABLE I. Parameters deduced from the complete fusion excitation function by a best fit of Eq. (3) to the data. The energy range is given in units of the barrier height V_0. χ^2 is calculated according to

$$\chi^2=\frac{1}{f}\sum_{n=1}^{N}\left(\frac{\sigma_{\exp.n}-\sigma_{\text{theor}.n}}{\Delta\sigma_n}\right)^2,$$

where N=number of data points, $f=N-3$, and $\Delta\sigma_n$ are the experimental uncertainties.

Reaction	Energy range	r_0 (fm)	V_0 (MeV)	$\hbar\omega$ (MeV)	χ^2
$^{35}Cl+^{58}Ni$	0.98–1.42	1.260 ± 0.03	61.3 ± 0.3	5.0 ± 1	1.13
$^{35}Cl+^{60}Ni$	0.97–1.33	1.28 ± 0.03	61.0 ± 0.3	7.4 ± 1	0.918
$^{35}Cl+^{62}Ni$	0.97–1.46	1.328 ± 0.03	60.8 ± 0.3	8.4 ± 1	0.198
$^{35}Cl+^{64}Ni$	0.97–1.39	1.334 ± 0.03	60.3 ± 0.3	8.0 ± 1	0.482

sion cross section as was done in Ref. 8. Assuming that both curvature $\hbar\omega_l$ and radius R_l are independent of the partial wave number l in the energy region considered here and that $V(R_l)$ differs from $V(R_0)=V_0$ only by the centrifugal term $\hbar^2 l(l+1)/2\mu R_0^2$, expressions (1) and (2) lead to

$$\sigma_{\text{cf}}=\frac{R_0^2\hbar\omega_0}{2E}\ln\left\{1+\exp\left[2\pi\left(\frac{E-V_0}{\hbar\omega_0}\right)\right]\right\}. \tag{3}$$

For $(E-V_0)>\hbar\omega_0$, Eq. (3) approaches the expression

$$\sigma_{\text{cf}}=\pi R_0^2\left(1-\frac{V_0}{E}\right) \tag{4}$$

of the sharp cutoff approximation.

Our data were used to fit R_0, V_0, and $\hbar\omega_0$ in Eq. (3). The energy region and the best-fit parameters are given in Table I. The parameters R_0 and V_0 follow a general trend in their mass dependence, which will be discussed elsewhere (Ref. 3). The resulting values for R_0 and V_0 were used to calculate σ_{cf} from Eq. (4). The result is given by the straight lines in Fig. 1. The size of the curvature $\hbar\omega_0$ is a criterion for the deviation from the sharp cutoff model. The parameter $\hbar\omega_0$ should be about constant for all four systems[9] as their quantum-mechanical properties, e.g. size and charge distribution, are nearly the same.[10] The extracted values of $\hbar\omega_0$, however, do vary strongly. Compared with liquid drop model calculations[9] the absolute value of $\hbar\omega_0$ is a factor of 2 to 3 too high.

One possible explanation is the influence of deformations. Static properties such as softness or quadrupole deformations of target and projectile are suggested to be of importance.[11] Wong[6] included static quadrupole deformations in the nuclear and Coulomb potential in the formalism given above but did neglect dynamic deformations.[12–14] Instead of a closed expression like Eq. (4), Wong obtained

$$\sigma_{\text{cf}}(E,\theta_1,\theta_2)=\frac{R_0^2\hbar\omega_0}{2E}\times\ln\left(1+\exp\left\{2\pi\left[\frac{E-V_0(\theta_1,\theta_2)}{\hbar\omega_0}\right]\right\}\right) \tag{5}$$

as the fusion cross section in head-on collisions. The θ_i are the angles or orientation, measured between the collision axis and the symmetry axis of the ith nucleus. $V_0(\theta_1,\theta_2)$ is the barrier height for this orientation. Neglecting the quadrupole-quadrupole term, $V_0(\theta_1,\theta_2)$ can be derived from the Coulomb and nuclear (Woods-Saxon) potential for deformed nuclei by introducing three additional parameters: the ground state deformation parameters $\beta_2^{(i)}$ $(i=1,2)$ and the nuclear radius para-

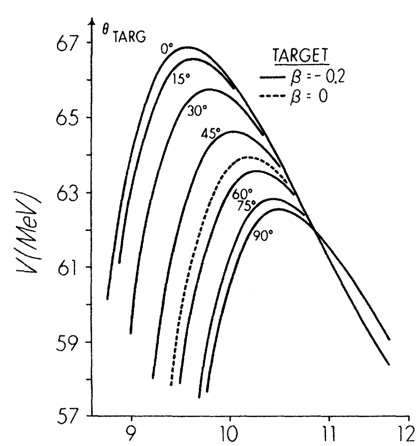

FIG. 3. Dependence of barrier position and height on the orientation of the deformed target nucleus. The barrier is the sum of a deformed Coulomb plus deformed real Wood-Saxon potential (parameter: $V_0=100$ MeV, $r_{0n}=1.2$ fm, $a=0.48$ MeV).

meter r_{0n} which is fixed to the value 1.2 fm throughout this work.

The barrier $V(\theta_1, \theta_2)$ varies quite considerably with the angle of orientation, even if one of the nuclei is spherical. Figure 3 demonstrates this dependence, which results in a slower decrease of the fusion excitation function at small energies compared with reactions between spherical nuclei.

The total fusion cross section may be derived from (5) by averaging over the different orientations. Vaz and Alexander[1] did this by considering a uniform distribution of barrier heights $V(\theta_1, \theta_2)$ between $\overline{V}_0 - \Delta$ and $\overline{V}_0 + \Delta$, where $\overline{V}_0$ is an average value. We rather follow the approach of Wong and use Eq. (5) together with solid angle weighting:

$$\langle \sigma_{\mathrm{cf}}(E) \rangle = \frac{1}{16\pi^2} \oint \oint \sigma_{\mathrm{cf}}(E, \theta_1, \theta_2) d\Omega(\theta_1) d\Omega(\theta_2). \quad (6)$$

This expression was fitted to our experimental data, using $\overline{V}_0$, R_0, $\hbar\omega_0$, and β_2^{Ni} as free parameters, $\beta_2(^{35}\mathrm{Cl})$ being fixed to -0.2 (Ref. 15).

In Fig. 4 data are compared to calculations (a) where deformation is neglected and (b) where de-

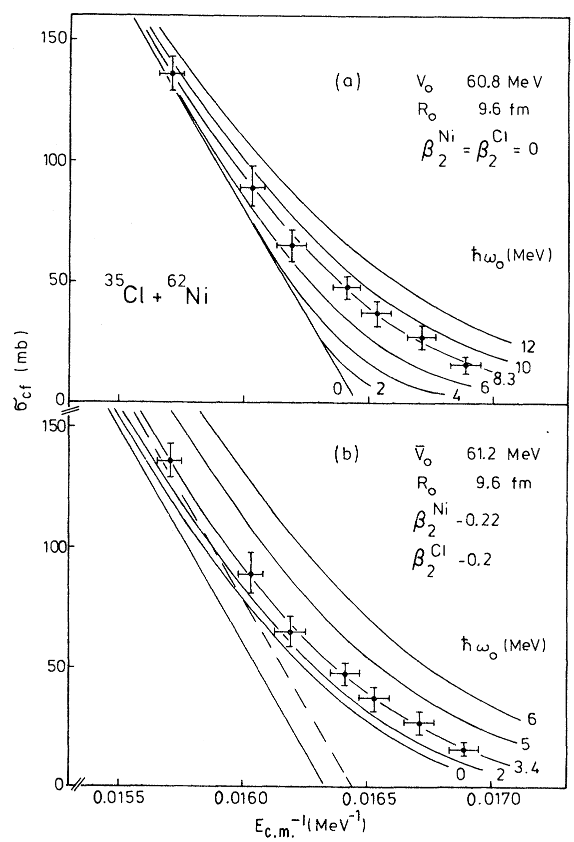

FIG. 4. Complete fusion cross sections $\sigma_{\mathrm{cf}}(E_{\mathrm{c.m.}}^{-1})$ for $^{35}\mathrm{Cl} + {}^{62}\mathrm{Ni}$ compared with (a) results of Eq. (3) and (b) results of Eq. (6). The dashed line in Fig. 3 (b) is identical with the $\hbar\omega_0 = 0$ result from Fig. 3 (a).

TABLE II. Three parameter fit results to experimental complete fusion data. In columns 2–6, search was done with $\hbar\omega_0$ kept fixed at 3 MeV; in columns 7–11, values for β_2^{Ni} were taken from Ref. 4.

Reaction	V_0 (MeV)	r_0 (fm)	$\hbar\omega_0$ (MeV)	β_2^{Ni}	χ^2	β_2^{Ni} [a]	V_0 (MeV)	r_0 (fm)	$\hbar\omega_0$ (MeV)	χ^2	$(BE2)$ β_2	$\hbar\omega_0$ Calc. (MeV) Ref. 16 Spher.	Def. [b]	Ref. 9 Spher.
$^{35}\mathrm{Cl} + {}^{58}\mathrm{Ni}$	61.58	1.272	3.0	−0.01	0.677	±0.0	61.4	1.262	2.3	0.628	+0.18	3.05	3.10	2.81
$^{35}\mathrm{Cl} + {}^{60}\mathrm{Ni}$	61.26	1.285	3.0	−0.179	0.606	−0.12	61.2	1.275	4.0	0.716	−0.2	3.01	3.01	2.77
$^{35}\mathrm{Cl} + {}^{62}\mathrm{Ni}$	61.12	1.328	3.0	−0.232	0.133	−0.15	61.4	1.328	5.2	0.152	−0.2	2.97	2.97	2.74
$^{35}\mathrm{Cl} + {}^{64}\mathrm{Ni}$	60.6	1.324	3.0	−0.225	0.413	−0.16	60.6	1.317	4.2	0.515	−0.17	2.94	2.93	2.71

[a] Hartree-Fock calculations, Ref. 4.
[b] Calculated $\beta_2^{\mathrm{Cl}} = -0.2$ (Ref. 15), $\beta_2^{\mathrm{Ni}} = \beta_2(BE2)$ (Refs. 17 and 18), and $\theta_1 = \theta_2 = 0°$.

formations are considered for both target and projectile. $\beta_2^{\mathrm{Ni}}=-0.22$ and $\hbar\omega_0=3.4$ MeV are the result of a four parameter fit to the data. While in both calculations V_0 and R_0 change by less than 1%, the value of $\hbar\omega_0$ is reduced from 8.3 to 3.4 MeV by taking deformations into account. As both parameters $\hbar\omega_0$ and β_2^{Ni} change the excitation function in a similar way it seems unreasonable to search for both simultaneously. Therefore, we present only three parameter best fits to the data where either $\hbar\omega_0$ or β_2^{Ni} was kept fixed.

In Table II, columns 2–6, the data are described with $\hbar\omega_0=3$ MeV, which corresponds to the value obtained from liquid drop model calculations,[16,9] columns 13 and 14. The best-fit values for β_2^{Ni} are in agreement with values derived from experimental $B(E2, 0^+\rightarrow 2^+)$ transition probabilities in the rigid spheroidal rotor model[17,18] (column 12), except for ^{58}Ni. The strong vibrator character of the Ni isotopes,[19] however, allows one only to extract an upper limit of the ground state deformation from $B(E2)$ values. The spherical shape found for ^{58}Ni is in especially good agreement with predictions from Hartee-Fock ground state deformation calculations,[4] column 7.

A three parameter search, based on these β_2^{Ni} values, yielded curvature parameters $\hbar\omega_0$ from 2.3 to 5.2 MeV, again reflecting the special character of ^{58}Ni (column 10).

IV. CONCLUSION

Thus, assuming a spherical ^{58}Ni and keeping in mind the approximations in the derivation of Eq. (6), one can consider the $\hbar\omega_0$ value of 3 MeV from liquid drop model calculations to be in good agreement with our data.

The approach [Eq. (6)] seems to be applicable in the energy range considered, i.e., down to a few MeV below the fusion barrier. At lower energies, however, the parabolic approximation of the barrier will fail.[20] In a first approximation the influence of deformation seems to be reasonably treated by taking into account only the static deformation of the nuclei involved. However, in a full treatment dynamical deformations should be included[14] which would reflect the difference in softness of the nuclei.

Obviously, one should do experiments where the probing nucleus is a spherical one. With the appropriate accelerator the investigation of fusion of ^{58}Ni with ^{58}Ni should allow one to extract the pure quantum-mechanical effect of barrier penetrability in fusion.

ACKNOWLEDGMENT

We are very grateful for the support and encouragement we obtained at Brookhaven National Laboratory, especially from Dr. A. Schwartzschild and Dr. H. E. Wegner, as well as for the hospitality during the performance of this experiment. We further thank Dr. D. Cline, Dr. D. Kolb, and Dr. R. Nix; and Dr. C. Y. Wong, who also made his program available to us, for stimulating and fruitful discussions.

---

*Present address: University of Hamburg, Hamburg, Germany.

[1]L. C. Vaz and J. M. Alexander, Phys. Rev. C 10, 464 (1974).

[2]J. M. Alexander, L. C. Vaz, and S. Y. Lin, Phys. Rev. Lett. 33, 1487 (1974).

[3]W. Scobel, A. Mignerey, M. Blann, and H. H. Gutbrod, unpublished.

[4]D. Kolb, R. Y. Cusson, and M. Harvey, Nucl. Phys. A150, 1 (1973); D. Kolb, R. Y. Cusson, and H. W. Schmitt, Phys. Rev. C 10, 1529 (1974); and D. Kolb, Gesellschaft für Schwerionenforschung, Darmstadt, private communication (unpublished).

[5]H. H. Gutbrod, W. G. Winn, and M. Blann, Nucl. Phys. A213, 267 (1973).

[6]C. Y. Wong, Phys. Rev. Lett. 31, 766 (1973).

[7]D. L. Hill and J. A. Wheeler, Phys. Rev. 89, 1102 (1953).

[8]H. Gauvin, Y. Le Beyec, M. Lefort, and R. L. Hahn, Phys. Rev. C 10, 722 (1974); and C. F. Tsang, Lawrence Berkeley Laboratory Report No. 2928, 1974 (unpublished).

[9]H. J. Krappe and J. R. Nix, in *Proceedings of the Third International Symposium on the Physics and Chemistry of Fission, Rochester 1973* (International Atomic Energy Agency, Vienna, 1974), Paper No. IAEA-SM-174/12; and private communication.

[10]H. Überall, *Electron Scattering from Complex Nuclei* (Academic, New York, 1971), Sec. 3, p. 204.

[11]J. O. Rasmussen and K. Sugawara-Tanabe, Nucl. Phys. A171, 497 (1971).

[12]A. S. Jensen and C. Y. Wong, Nucl. Phys. A171, 1 (1971).

[13]H. Holm and W. Greiner, Phys. Rev. Lett. 24, 404 (1970).

[14]P. W. Riesenfeld and T. D. Thomas, Phys. Rev. C 2, 711 (1970).

[15]G. H. Fuller and V. W. Cohen, Nucl. Data A5, 433 (1969).

[16]R. Bass, Nucl. Phys. A231, 45 (1974); and Phys. Lett. 29, 139 (1973).

[17]P. H. Stelson and L. Grodzins, Nucl. Data A1, 21

(1967).
[18]A. Christie and O. Häusser, Nucl. Data A11, 281 (1973).
[19]P. M. S. Lesser, D. Cline, C. Kalbach-Cline, and A. Bahnsen, Nucl. Phys. A223, 563 (1974).
[20]H. Freiesleben and J. Huizenga, Nucl. Phys. A224, 503 (1974).